ARTICLES

A Direct ab-Initio Trajectory Study on the Ionization Dynamics of the Water Dimer

Hiroto Tachikawa*

Division of Molecular Chemistry, Graduate School of Engineering, Hokkaido University, Sapporo 060-8628, Japan

Received: April 2, 2002; In Final Form: May 29, 2002

Ionization processes of a water dimer have been investigated by means of full dimensional direct ab-initio trajectory method. The structure of $(H_2O)_2$ before the ionization was simulated at 10 K up to 2 ps by means of a direct ab-initio molecular dynamics (MD) method. Sixty geometrical configurations were selected from the MD calculation, and then the dynamics of $(H_2O)_2^+$ were calculated by means of a direct ab-initio trajectory method under a constant energy condition. The trajectories on two electronic state potential energy surfaces of $(H_2O)_2^+$, i.e., the $^2A''$ and $^2A'$ states, were full-dimensionally calculated under the C_s symmetry. For the $^2A''$ state, a complex composed of H_3O^+ and OH, which is expressed by $(H_3O^+)OH$, was only formed as a long-lived complex. On the other hand, in the ionization to the $^2A'$ state, two reaction channels, the complex formation $(H_3O^+)OH$ ($^2A'$) and direct dissociation ($H_3O^+ + OH$) were open as product channels. The dynamics calculations indicated that the proton of H_2O^+ transferred to H_2O within 100−150 fs for the $^2A''$ state, whereas the proton transfer at the $^2A'$ state occurs faster (30−50 fs) than that of the $^2A''$ state. The mechanism of the ionization dynamics of $(H_2O)_2$ was discussed on the basis of theoretical results.

1. Introduction

In the ionization of an isolated molecule, the structural relaxation of the ion occurs as a main decay process.[1] On the other hand, in the case of the ionization of complex, dimer, and clusters,[2−6] there are several decay processes as schematically expressed by

$$A(H_2O)_n + h\nu \rightarrow [A^+(H_2O)_n]_{ver} + e^- \quad \text{ionization}$$

$$[A^+(H_2O)_n]_{ver} \rightarrow A^+ + (H_2O)_n \quad \text{dissociation}$$

$$\rightarrow A^+(H_2O)(H_2O)_{n-1} \quad \text{complex formation}$$

$$\rightarrow A^+H + (OH)(H_2O)_{n-1} \quad \text{proton or hydrogen transfer}$$

where A is a molecule in water cluster, and $[A^+(H_2O)_n]_{ver}$ means a hydrated A^+ ion at a vertical ionization point. The first channel expresses the dissociation process following the ionization of $A(H_2O)_n$. The second is a complex formation channel in which A^+ binds strongly to one or two water molecules in the water cluster. In the third channel, proton or hydrogen atom transfer occurs between A^+ and the water cluster. These three channels would be competitive with each other after the ionization of $A(H_2O)_n$.

The water dimer is one of the simplest molecular complexes.[7,8] The ionization dynamics of the water dimer have been investigated experimentally by Ng and co-workers in detail.[9] They measured the photoionization efficiency curve of the water dimer and water clusters by means of photoionization mass spectrometry (PIMS) method, and showed that the ionization potential of the water dimer is 11.21 ± 0.09 eV which is largely lower than that of water monomer (I_p = 12.62 ± 0.02 eV). Also, it was found that the PIMS curve for the ionization of the water dimer is not clearly increased around the threshold region. Thus, the shape of the PMIS curve of $(H_2O)_2$ is much different from that of the water monomer. This feature is one of the interesting points in this system.

Tomoda et al. determined the vertical (I_v) and the threshold (I_{th}) ionization energy of the water dimer by means of molecular-beam photoelectron spectroscopy.[10] The first and second ionization potentials (I_v's) were measured by 12.1 and 13.2 eV, respectively. I_{th} of $(H_2O)_2$ was measured to be 11.2 eV. They also carried out ab-initio molecular orbital (MO) calculations for $(H_2O)_2$ and $(H_2O)_2^+$. The potential energy surface for $(H_2O)_2^+$ showed that $(H_2O)_2^+$ forms the $H_3O^+(OH)$ complex spontaneously. Thus, the static properties of $(H_2O)_2^+$ have been extensively accumulated from experimental points of view.

Bartnett and Landman[11] investigated the ionization dynamics of $(H_2O)_2$ by means of the Born−Oppenheimer local-spin-density functional molecular dynamics (BO-LSD-MD) method. They suggested that the proton-transfer undergoes a fast barrierless auto-protonation process (the estimated rate was about 50 fs). However, details of the dynamical mechanism of the ionization of $(H_2O)_2$ are not completely understood. In particular, the ionization dynamics on two electronic states ($^2A''$ and $^2A'$) were little known, although the water dimer has two ionization states, $^2A''$ and $^2A'$, as low-lying ionic states.

In the present study, direct ab-initio dynamics calculations have been applied to the ionization dynamics of $(H_2O)_2$. The purposes of this study are to elucidate the ionization processes

10.1021/jp020871q CCC: $22.00
Published on Web 06/27/2002

of $(H_2O)_2$ from a theoretical point of view, and to estimate the reaction time for the proton transfer between H_2O^+ and H_2O in the water dimer. In a previous paper, we investigated the ionization dynamics of the $(CH_3OH)_2$ methanol dimer by means of the direct ab-initio trajectory method.[12] It was found that the complex composed of $(CH_3OH_2^+)(CH_3O)$ is formed only following the ionization of the methanol dimer. In the present work, a similar method would apply to the ionization dynamics of the water dimer.

2. Method of Calculation

The present reaction system $(H_2O)_2$ has a large number of degrees of freedom ($3N - 6 = 12$), so that it is quite difficult to fit the ab-initio surface to analytical functions of the interatomic potential. Hence, direct ab-initio dynamics calculation[13−15] is the best way to treat the reaction dynamics for the present reaction system. In this work, we used a direct ab-initio dynamics calculation using full dimensional potential energy surface. The calculations were carried out at the HF/6-311G(d,p) level of theory. Details of the methods of the calculations were described elsewhere.[13,14]

The direct ab-initio molecular dynamics (MD) calculations were carried out at the HF/6-311G(d,p) level of theory throughout. First, a trajectory of neutral system $(H_2O)_2$ was run at a constant temperature in order to obtain the structures at finite temperature. The optimized structure of $(H_2O)_2$ obtained at the HF/6-311G(d,p) level was chosen as the initial structure. At the start of the trajectory calculation, atomic velocities are adjusted classically to give a mean temperature of 10 K. Temperature of the system is defined by

$$T = \frac{1}{3kN}\langle \sum_i m_i v_i^2 \rangle \tag{1}$$

where N is number of atoms, v_i and m_i are velocity and mass of ith atom, and k is Boltzmann's constant. To keep the constant mean temperature of $(H_2O)_2$, we used a simple scheme for constant temperature simulation.[16] Bath relaxation time (τ) was fixed to $\tau = 0.01$ ps during the simulation.

Second, a total of 60 geometrical configurations were randomly selected from those calculated by the ab-initio MD calculation at 10 K. And then, 60 trajectories on the ionic state PESs of $(H_2O)_2^+$ were run on the assumption of vertical ionization from neutral dimer. The trajectory calculations of $(H_2O)_2^+$ were performed under a constant total energy condition. The velocities of atoms at the starting point were assumed to be zero (i.e., the momentum vector of each atom is zero). The equations of motion for n atoms in a molecule are given by

$$\frac{dQ_j}{dt} = \frac{\partial H}{\partial P_j}$$

$$\frac{\partial P_j}{\partial t} = -\frac{\partial H}{\partial Q_j} = -\frac{\partial U}{\partial Q_j} \tag{2}$$

where $j = 1-3N$, H is classical Hamiltonian, Q_j is the Cartesian coordinate of the jth mode, and P_j is the conjugated momentum. These equations were numerically solved by the Runge−Kutta method. No symmetry restriction was applied to the calculation of the gradients in the Runge−Kutta method. The time step size was chosen by 0.10 fs, and a total of 10 000 steps were calculated for each dynamics calculation. The drift of the total energy is confirmed to be less than 0.1% throughout at all steps in the trajectory. The momentum of the center of mass and the angular momentum are assumed to be zero. Static ab-initio MO calculations were carried out using Gaussian 98 program package using 6-311G(d,p) basis sets[17] in order to obtain more accurate energetics.

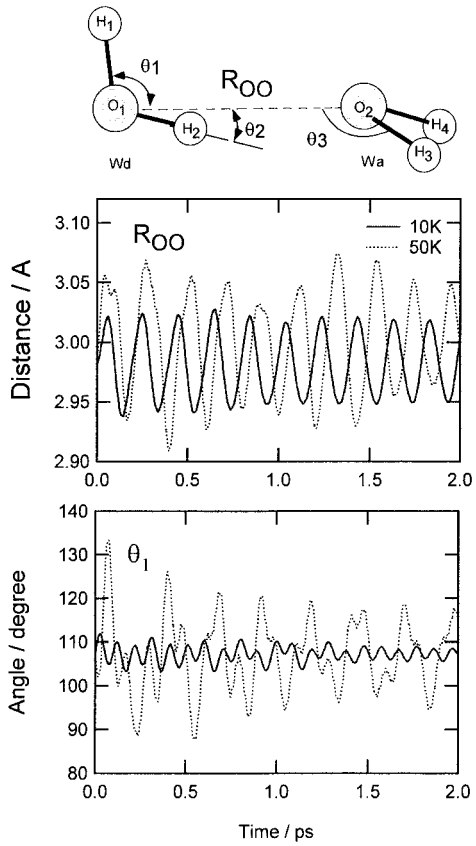

Figure 1. Result of the ab-initio molecular dynamics (MD) calculation for neutral water dimer at 10 and 50 K. Time dependence of the oxygen−oxygen distance (R_{OO}) of water molecules (A) and angle of θ_1 (B). The geometrical parameters and schematic structure of the water dimer are also illustrated (upper).

3. Results

A. Structures of $(H_2O)_2$ at 10 K. First, a trajectory of neutral linear form dimer was calculated in order to obtain the structure of $(H_2O)_2$ at finite temperature. We chose 10 and 50 K as simulation temperatures and the optimized structure obtained by HF/6-311G(d,p) calculation as the initial structure of the water dimer. Details of the structures and electronic states of $(H_2O)_2$ and $(H_2O)_2^+$ will be described in Section 3E.

The results for the direct ab-initio MD calculations for 10 K were given in Figure 1. Wd and Wa in the upper panel refer to the water molecule as a proton-donor and acceptor in the water dimer, respectively. The oxygen−oxygen distance (R_{OO}) of $(H_2O)_2$, which is defined by a O_1-O_2 distance, largely oscillated in the range from 2.93 to 3.02 Å at 10 K. Also, the angle (θ_1) fluctuated in the range 103−112°. These results indicate that the neutral dimer has a very nonrigid structure at low temperature and has a wide Franck−Condon region. For comparison, the same calculation was carried out at 50 K. The distance R_{OO} and the angle θ_1 largely vibrated in the range 2.91−3.07 Å and 90−125°, respectively. However, at both temperatures (10 and 50 K), the hydrogen bond was not broken by thermal activation.

B. Ionization Dynamics of $(H_2O)_2$ on the $^2A''$ State Surface. The water dimer cation has the $^2A''$ and $^2A'$ states as low-lying ionization states.[9,10] Hence, in the present calculations, the relaxation processes of $(H_2O)_2^+$ from two electronic states

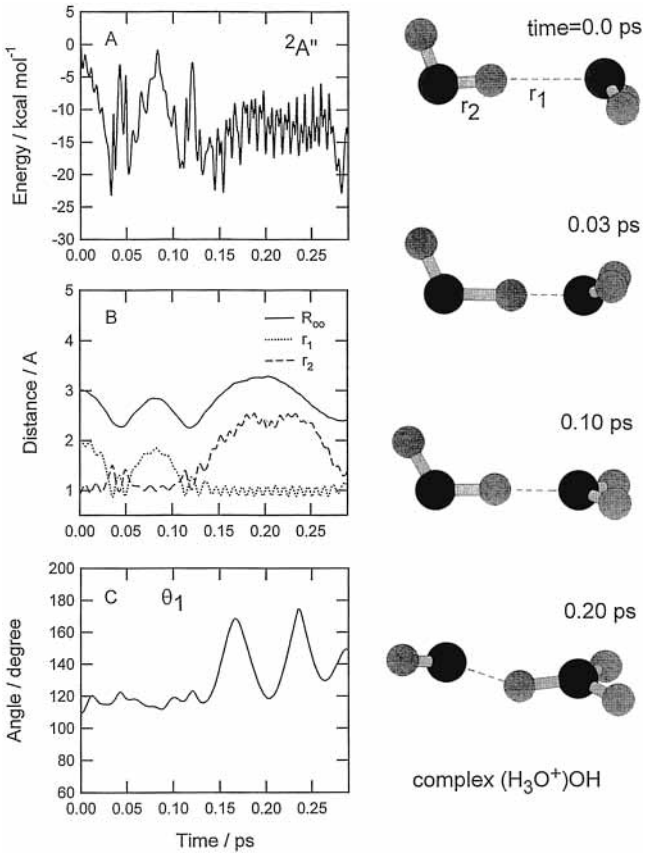

Figure 2. A sample trajectory for $(H_2O)_2^+$ on the $^2A''$ state potential energy surface following the vertical ionization of water dimer. The energy of the system (A), bond distances (B), and angle (θ_1) plotted as a function of reaction time.

($^2A''$ and $^2A'$) were considered in the calculations. In the $^2A''$ state, which is the lowest ionization state of the water dimer, the electron is removed from the n_π orbital of Wd which possesses a nonbonding orbital perpendicular to the C_s molecular plane. On the other hand, the electron is removed from the n_σ-orbital located on the molecular plane at the $^2A'$ state. In the present ab-initio MD and trajectory calculations, we considered C_s symmetry in the calculation.

A sample trajectory for $(H_2O)_2^+$ on the $^2A''$ state surface, ionized vertically from the neutral water dimer, was given in Figure 2. At time zero, the trajectory was vertically shifted from the neutral state to the $^2A''$ state by the ionization of $(H_2O)_2$. A hole was localized in the n_π orbital in the out-of-plane which is perpendicular to the C_s molecular plane. The energy of the system was stabilized rapidly by about 5 kcal/mol which is caused by the deformation of H_2O (Wd) by the ionization: the H−O−H angle was varied from 105° to 120° after the ionization. The water cation (Wa) collided first with the water molecule (Wd) at 0.03 ps, but the proton transfer did not occur here. The second collision occurred at time 0.12 ps. At this point, the proton was transferred from H_2O^+(Wd) to H_2O(Wa). This process was clearly seen in Figure 2B as time dependence of r_1 and r_2: namely, the distances were exchanged with each other at time = 0.12 ps.

Figure 2 (right) shows snapshots of $(H_2O)_2^+$ ($^2A''$) after the ionization of $(H_2O)_2$. At time zero, the structure of $(H_2O)_2^+$ corresponds to that of the neutral water dimer with a linear form. After the ionization to the $^2A''$ state, the possible hole was localized in the n_π orbital of Wd. The proton was quickly transferred to the oxygen of Wa after several vibrations between OH and H_2O. The complex composed of $(H_3O^+)OH$ was spontaneously formed after the ionization of $(H_2O)_2$ to the $^2A''$ state. The lifetime of the complex was longer than at least 2−5 ps, and it is long enough to observe experimentally as an intermediate long-lived complex.

C. Ionization Dynamics of the Water Dimer: Dynamics on the $^2A'$ State. For the ionization to the $^2A'$ state, two reaction channels were found as decay processes of $(H_2O)_2^+$. One is a dissociation channel in which the complex $(H_3O^+)OH$ is directly dissociated into $H_3O^+ + OH$. The other one is a complex formation channel in which a long-lived complex $(H_3O^+)OH$ ($^2A'$) is formed after the ionization of the water dimer. First, we would explain the former reaction channel (dissociation) here.

A hole is localized mainly in the n_σ orbital of Wd by the ionization to the $^2A'$ state. After the ionization, the energy of the system decreased suddenly to −20 kcal/mol because of a rapid deformation of H−O−H angle of Wd and a rapid proton movement (Figure 3A). This structural change was also seen in the time dependence of angle θ_1 (Figure 3C): the angle increased suddenly from 105° to 180°. The proton of Wd was rapidly transferred to the oxygen of Wa before the oxygen atom of Wd approached Wa. Figure 3B showed that the distances r_1 and r_2 cross each other at time 20 fs, suggesting that the proton of Wd was transferred at this point, and subsequently the oxygen of Wd collided to Wa at 50 fs. After that, the OH radical was separated from H_3O^+. From time dependence of r_2 (Figure 3B) and θ_1 (Figure 3C), it was clearly indicated that the OH radical rotated quickly after the dissociation. The time period of the rotation was estimated to be about 50 fs from Figure 3C.

Snapshots of the conformation of the water dimer after the ionization were illustrated in Figure 3 (right). At time 30 fs, the proton in Wd was rapidly transferred to Wa, and the (H_3O^+)-OH complex was formed. However, the complex was quickly dissociated into $H_3O^+ + OH$ within a very short lifetime. At 150 fs, the OH radical went away from H_3O^+. Thus, the dissociation occurs as a very fast process at the $^2A'$ state.

The result for the complex formation channel was given in Figure 4. After the ionization, the proton was rapidly transferred to Wa as well as in the dissociation channel. After the proton transfer, the OH radical separated from H_3O^+ at once, but it has returned again at $R_{OO} = 4.0$ Å. At the final state, the long-lived complex was formed. A snapshot also showed such a situation in the complex formation. The excess energy was dissipated mainly into the OH bending mode and an intermolecular vibrational mode between H_3O^+ and OH.

D. Comparison of the Potential Energies for Two States. To compare time dependence of the energies for the reaction systems on two electronic states, the potential energies for two ionization states, the $^2A''$(lower curve) and $^2A'$ (upper curve) states, were plotted in Figure 5 as a function of reaction time. At time zero, the energies for the $^2A''$ and $^2A'$ states were calculated to be −151.7331 au and −151.6521 au, respectively, indicating that the vertical ionization point for the $^2A'$ state was 2.2 eV higher in energy than that of the $^2A''$ state. The energy for the $^2A''$ state was almost lower than that of the $^2A'$ state during the reaction. At 20 fs, the upper curve was slightly lower than that of the $^2A''$ state, suggesting that the complex (H_3O^+)-OH ($^2A'$) is formed in this region. However, its lowest point of the $^2A'$ state at time = 20 fs was slightly higher in energy than that of the $^2A''$ state corresponding to the $(H_3O^+)OH$ ($^2A''$) complex at time = 30 fs. As clearly seen in Figure 5, change of the energy for the $^2A'$ state is more striking than that of the $^2A''$ state. The time regions for the proton transfer were indicated by horizontal lines in Figure 5. The proton transfer at the $^2A'$

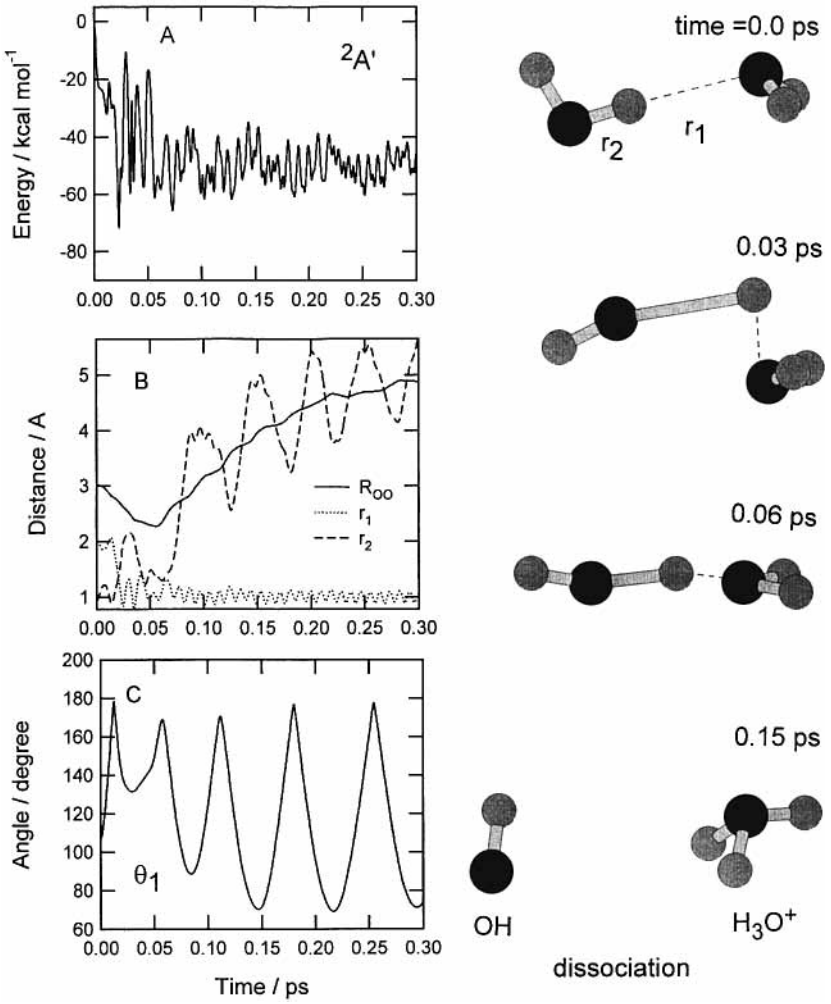

Figure 3. A sample trajectory for dissociation channel of $(H_2O)_2^+$ on the $^2A'$ state potential energy surface following the vertical ionization of water dimer. The energy of the system (A), bond distances (B), and angle (θ_1) plotted as a function of reaction time.

state occurred much faster than that of the $^2A'$ state. From a number of 60 trajectories, the branching ratio for complex and dissociation channels was estimated roughly to be about 2:1, respectively. However, larger numbers of trajectories need in order to obtain more accurate branching ratio.

E. Potential Energy Surfaces. The two-dimensional potential energy surface ($^2A''$ state) calculated at the MP4SDQ/6-311G-(d,p) level was given in Figure 6 (upper panel). The energy minimum corresponding to the complex $(H_3O^+)OH$ ($^2A''$) was found at $r_1 = 1.05$ Å and $r_2 = 1.47$ Å. From the shape of PES, it was shown that the valley is open for the direction of product $H_3O^+ + OH$. PES calculated at the HF/6-311G(d,p) was illustrated in Figure 6 (lower panel) for comparison. The shape of PES calculated by the HF method was in excellent agreement with that of MP4SDQ method. This implies that the HF calculation would give a reasonable feature for the ionization dynamics of $(H_2O)_2$. The fully optimized parameters of the $(H_3O^+)OH$ complexes at the $^2A''$ and $^2A'$ states were given in Table 1. From these structural parameters, it was suggested that the complex was composed of the H_3O^+ ion and the OH radical. This structure is also supported by a simple Mulliken population of the complex that the unpaired electron was mainly distributed in the OH radical. The $(H_3O^+)OH$ ($^2A''$) was slightly more stable in energy than that of the $^2A'$ state. The energy differences were calculated to be 2.6 kcal/mol at the QCISD/6-311G(d,p) level. The HF/6-311G(d,p) calculations gave similar features of the structures and energetics for the complexes.

TABLE 1: Optimized Parameters of $(H_3O^+)OH$ Complex at the $^2A''$ and $^2A'$ States Calculated at the QCISD/6-311G(d,p) and HF/6-311G(d,p) (Bond distances and angles are in Å and in degrees, respectively)

	QCISD		HF	
	$^2A''$	$^2A'$	$^2A''$	$^2A'$
R_1	1.0516	1.0057	1.0024	0.9836
R_2	1.4235	1.5199	1.5480	1.5998
θ_1	122.2	179.8	131.6	179.9
θ_2	0.0	0.0	0.0	0.0
θ_3	122.2	121.0	121.2	120.7

4. Discussion

A. Model of the Ionization of the Water Dimer. In the present paper, the ionization dynamics of the water dimer have been investigated by means of direct ab-initio trajectory methods. Two electronic states, $^2A''$ and $^2A'$ states, were considered as potential energy surfaces for the decay processes of $[(H_2O)_2^+]_{ver}$, where $[(H_2O)_2^+]_{ver}$ means the water dimer cation at the vertical ionization point from the neutral water dimer.

For the $^2A''$ state (an electron is removed from the n_π orbital perpendicular to the molecular C_s plane), all trajectories gave the long-lived complex composed of $(H_3O^+)OH$. The proton of Wd was directly transferred to the oxygen of Wa after several vibrations of the hydrogen atom between OH and H_2O. On the other hand, for the $^2A'$ state (an unpaired electron is located in the n_σ orbital on the molecular plane), two reaction channels were found. One of the channels is complex formation in which

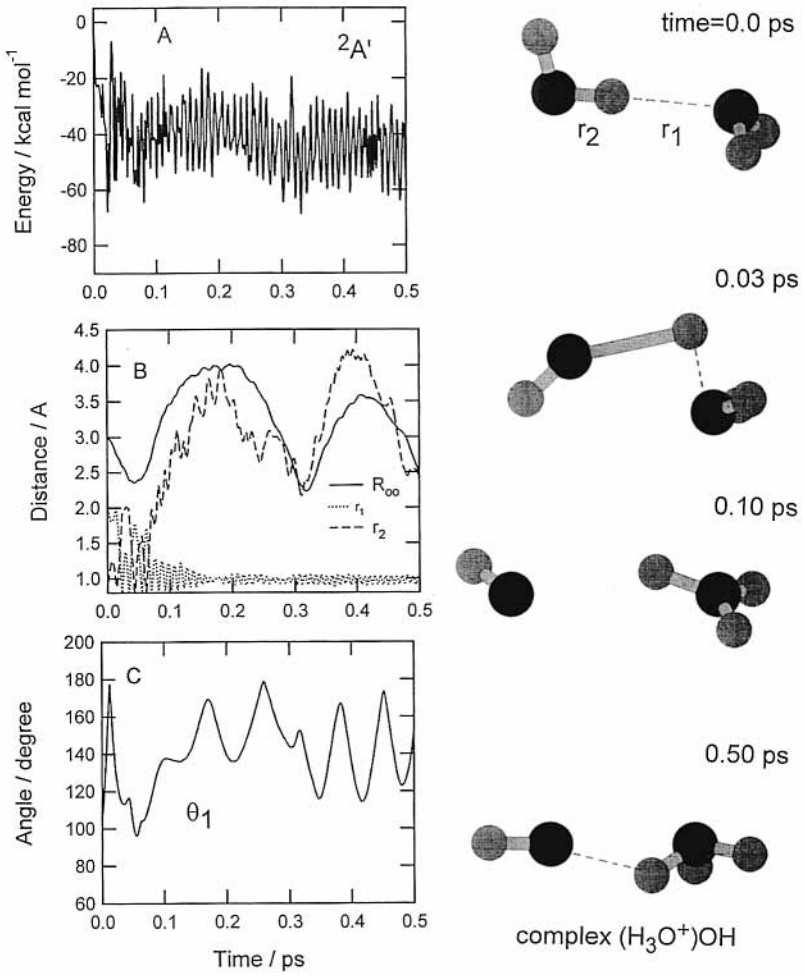

Figure 4. A sample trajectory for complex formation channel of $(H_2O)_2^+$ on the $^2A'$ state potential energy surface following the vertical ionization of the water dimer. The energy of the system (A), bond distances (B), and angle (θ_1) plotted as a function of reaction time.

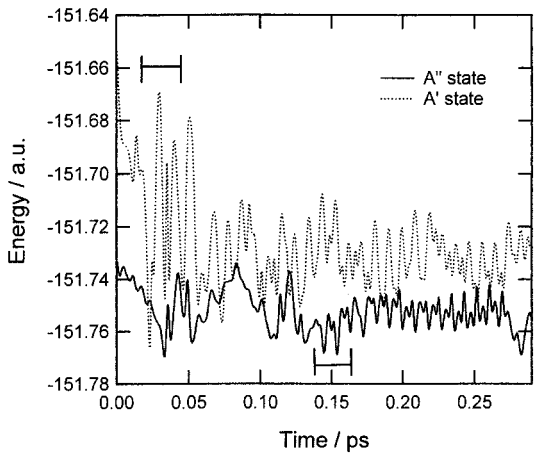

Figure 5. Potential energies of the reaction systems for the $^2A''$ (solid curve) and $^2A'$ (dashed curve) states plotted as a function of reaction time.

the proton of H_2O^+ (Wd) is transferred directly into the H_2O molecule (Wa). This channel is very similar to that of (H_3O^+)-OH at the $^2A''$ state, but the rate of the proton transfer is much faster than that of the $^2A''$ state. Also, the electronic states of the complexes are different from each other. Those are (H_3O^+)-OH ($^2A''$) and $(H_3O^+)OH$ ($^2A'$). The other channel is dissociation in which H_3O^+ (X^1A_1) and OH ($^2\Pi$) are separated from each other after the ionization of $(H_2O)_2$. The reaction occurs via the $(H_3O^+)OH$ ($^2A'$) complex region on the $^2A'$ surface, although the lifetime is negligibly short.

As a summary of the present calculations, a reaction model is proposed here. Potential energy curves for the ionization processes of water dimer were schematically illustrated in Figure 7. The lower curve indicates PEC for the neutral water dimer illustrated as a function of intermolecular distance. There are two low-lying ionization states at the water dimer cation. The $^2A''$ state is slightly higher in energy than that of dissociation limit ($H_3O^+ + OH$), but the excess energy is mostly distributed into the internal modes of $(H_3O^+)OH$. Therefore, almost all trajectories lead to the complex formation. The $^2A'$ state is higher energy than the dissociation limit. Hence, both the dissociation product ($H_3O^+ + OH$) and complex formation were found. In the former case, the rotational excitation of the OH radical is predicted by the present calculations. On the other hand, in the latter case, the excess energy is dissipated mostly into the internal modes of the complex.

B. Comparison with Previous Experiments. From the HeI photoelectron spectrum of the water dimer, Tomoda et al.[4] obtained the first two vertical ionization energies (12.1 ± 0.1 eV and 13.2 ± 0.2 eV) and a threshold ionization energy (11.1 eV) which is in good agreement with the photoionization threshold (11.21 ± 0.09 eV) by Ng et al. Also, Ng et al.[9] measured the first appearance potential of $(H_2O)_2^+$ to be 11.21 eV, and the H_3O^+ ion was found as the product ion at 11.73 eV. The present calculations indicated that the ionization to the $^2A'$ state leads to the complex formation $(H_3O^+)OH$ ($^2A''$), and

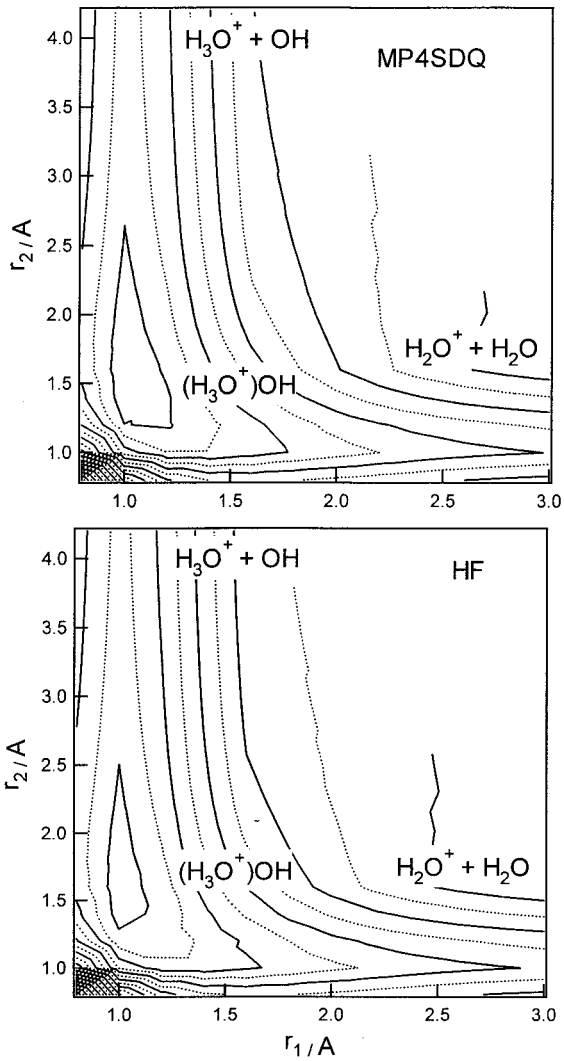

Figure 6. Potential energy surfaces calculated as functions of r_1 and r_2 of $(H_2O)_2^+$ (^{2}A" state) calculated at (upper panel) MP4SDQ/6-311G-(d,p) and (lower panel) HF/6-311G(d,p) levels of theory. Contours are plotted by each 0.02 au.

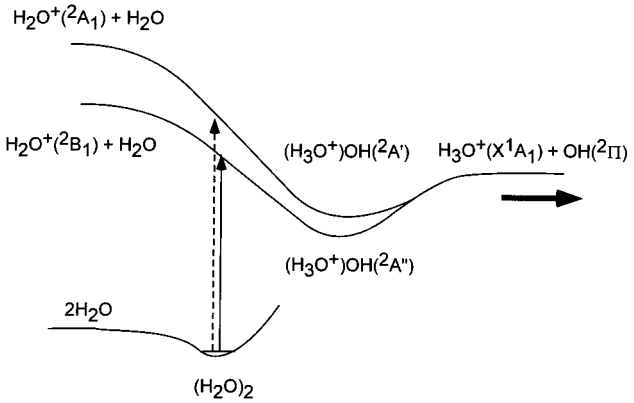

Figure 7. One-dimensional potential energy surfaces for the ionization of the water dimer. Upper and lower curves are schematically illustrated for the ionization states (^{2}A″ and ^{2}A′ states) and neutral state, respectively. Allows indicate the vertical ionization from the neutral state.

that to the ^{2}A′ state leads to two reaction channels, dissociation ($H_3O^+ + OH$) and complex formation $(H_3O^+)OH$ (^{2}A′). Also, our calculations suggested that the product $(H_2O)_2^+$ was formed at the ^{2}A″ state, while formation of H_3O^+ is possible to the ionization to the ^{2}A′ state.

C. Comparison with Previous Theoretical Studies. Previous theoretical calculations predicted that the ionization of water dimer causes the fast proton transfer occurring as a reaction $(H_2O)_2^+ \rightarrow (H_3O^+)OH$.[10,11] The present calculations also support previous theoretical results. In the present study, the rates of the proton-transfer processes for the ^{2}A″ and ^{2}A′ states were calculated to be 100−150 fs and 30−50 fs, respectively, suggesting that the proton transfer of the ^{2}A′ state is much faster than that of the ^{2}A″ state. This is due to the fact that the positive charge is fully localized on the transferring proton of Wd at the ^{2}A′ state at time zero. On the other hand, several collisions are required in the proton transfer at the ^{2}A″ state. Thus, the present study elucidates details of the ionization of water dimer.

In 1983, Tomoda and Kimura[18] calculated the potential energy surfaces for the proton-transfer reactions in the ^{2}A″ and ^{2}A′ states of $(H_2O)_2^+$. From the calculations of PESs, it was found that the structure of the water dimer cation is largely distorted from that of neutral dimer. Also, they indicated that the proton transfer occurs without activation barrier. The vertical ionization points from the equilibrium structure of the water dimer on both PESs are lower in energy than that of the dissociation limit ($H_2O^+ + H_2O$), but are higher than that of the proton-transferred product ($H_3O^+ + OH$). These features are in good agreement with that obtained by more accurate calculations in the present study. The present dynamics calculations support strongly their prediction derived from their calculations and experiments.

As a structure of the water dimer cation, a hydrazine-like structure was proposed on the basis of ab-initio calculations.[11,19] This structure is composed of $(H_2O-OH_2)^+$ where the oxygen atoms bind each other in the cluster and positive charge is fully delocalized on the complex. In the present dynamics calculations, however, the water dimer cation, having a structure composed of the H_3O^+ ion and the OH radical, was obtained only after the ionization of the linear form water dimer. The hydrazine-type cation may be formed accidentally by the bimolecular reaction of H_2O^+ with H_2O.

D. Additional Comments. We have introduced several approximations to calculate the potential energy surface and to treat the reaction dynamics. First, we assumed that $[(H_2O)_2^+]_{ver}$ has no excess energy at the initial step of the trajectory calculation (time = 0.0 ps). This may cause a change of lifetime and energy distribution of the products. In the case of higher excess energy, the $[(H_2O)_2^+]_{ver}$ complexes dissociate more easily into $H_3O^+ + OH$. However, this effect was not considered in the present calculations. It should be noted therefore that the present model is limited in the case of no excess energy. Also, we assumed that initial momentum vectors of atoms are zero at time zero. However, this approximation would be adequate to treat the dynamics because the energy gradients of atoms on PES of the dimer cation are larger than the momentum vectors of atoms.

Second, we assumed that electronic state of $(H_2O)_2^+$ keeps itself during the reaction. This means that electronic transition probability between $(H_2O)_2^+$ (^{2}A″ and ^{2}A′) is assumed to be zero. Therefore, we monitored carefully whether the electronic state is held in the running the trajectory. In the results given in the present paper, all trajectories kept their own electronic state. Therefore, there is no problem for instability of the electronic state during the trajectory. However, CASSCF−CI dynamics may be required in order to more detailed information. The surface hopping, which is completely neglected in the present study, may be important to gain the whole ionization

processes of the water dimer. However, these calculations represent future work, so that we do not make refer to them any more.

Last, we assumed HF/6-311G(d,p) multidimensional potential energy surface in the trajectory calculations throughout. As mentioned in Section 3, this level of theory represents reasonably a potential energy surface obtained by the MP4SDQ calculation. Also, it is in good agreement with the QCISD calculations. Therefore, the level of theory used in the present calculation would be adequate to discuss qualitatively the ionization dynamics of the water dimer.

The binding energies of the complex (H_3O^+OH) relative to the dissociation limit ($H_3O^+ + OH$) are calculated at the HF/6-311G(d,p) level to be −19.0 kcal/mol ($^2A''$ state) and −18.3 kcal/mol ($^2A'$ state). The QCISD/6-311G(d,p) calculations gave −21.6 ($^2A''$ state) and −19.0 kcal/mol ($^2A'$ state), indicating that the HF calculation would give a shallow trapping energy. This may cause a slight change of a lifetime of the complex. More accurate wave functions may provide deeper insight into the dynamics. Such a calculation will be possible after development of a high-speed CPU computer in near future. Despite the several assumptions introduced here, the results enable us to obtain valuable information on the mechanism of the ionization of the water dimer.

Acknowledgment. The author is indebted to the Computer Center at the Institute for Molecular Science (IMS) for the use of the computing facilities. I also acknowledge partial support from a Grant-in-Aid from the Ministry of Education, Science, Sports and Culture of Japan.

References and Notes

(1) Kimura, K.; Katsumata, S.; Achiba, Y.; Yamazaki, T.; Iwata, S. In *Handbook of HEI Photoelectron Spectra of Fundamental Organic Molecules*; Japan Scientific Societies Press: Tokyo, 1981.
(2) Müller-Dethlefts, K.; Dopfer, O.; Wright, T. G. *Chem. Rev*. **1994**, *94*, 1845.
(3) Zwier, T. S. *Annu. Rev. Phys. Chem*. **1996**, *47*, 205.
(4) Tomoda, S.; Kimura, K. In *Vacuum Ultraviolet Photoionization and Photodissociation of Molecules and Clusters*; Ng, C.-Y., Ed.; World Scientific, 1991; Chapter 3, pp 101−161.
(5) Tachikawa, H.; Igarashi, M. *J. Phys. Chem.* **1998**, *102*, 8648.
(6) Tachikawa, H. *J. Phys. Chem. A* **1999**, *103*, 6873.
(7) Dyke, T. R.; Mack, K. M.; Muenter, J. S. *J. Chem. Phys*. **1977**, *66*, 498.
(8) Morokuma, K.; Pedersen, L. *J. Chem. Phys.* **1968**, *68*, 3275.
(9) Ng, C.-Y. *Adv. Chem. Phys.* **1983**, *52*, 263.
(10) Tomoda, S.; Achiba, Y.; Kimura, K. *Chem. Phys. Lett.* **1982**, *87*, 197.
(11) Bartnett, R. N.; Landman, U. *J. Phys. Chem*. **1995**, *99*, 17305.
(12) Tachikawa, H. *Chem. Phys.* **1999**, *244*, 263.
(13) Tachikawa, H. *J. Phys. Chem. A* **2001**, *105*, 1260.
(14) Tachikawa, H. *J. Phys. Chem. A* **2000**, *104*, 7738.
(15) Vreven, T. *J. Am. Chem. Soc*. **1997**, *119*, 12687.
(16) Berendsen, H. J. C.; Postma, J. P. M.; Van Gunsteren, W. F.; di Nola, A.; Haak, J. P. *J. Chem. Phys.* **1984**, *81*, 3684.
(17) Frisch, M. J.; Trucks, G. W.; Schlegel, H. B.; Scuseria, G. E.; Robb, M. A.; Cheeseman, J. R.; Zakrzewski, V. G.; Montgomery, J. A., Jr.; Stratmann, R. E.; Burant, J. C.; Dapprich, S.; Millam, J. M.; Daniels, A. D.; Kudin, K. N.; Strain, M. C.; Farkas, O.; Tomasi, J.; Barone, V.; Cossi, M.; Cammi, R.; Mennucci, B.; Pomelli, C.; Adamo, C.; Clifford, S.; Ochterski, J.; Petersson, G. A.; Ayala, P. Y.; Cui, Q.; Morokuma, K.; Malick, D. K.; Rabuck, A. D.; Raghavachari, K.; Foresman, J. B.; Cioslowski, J.; Ortiz, J. V.; Stefanov, B. B.; Liu, G.; Liashenko, A.; Piskorz, P.; Komaromi, I.; Gomperts, R.; Martin, R. L.; Fox, D. J.; Keith, T.; Al-Laham, M. A.; Peng, C. Y.; Nanayakkara, A.; Gonzalez, C.; Challacombe, M.; Gill, P. M. W.; Johnson, B. G.; Chen, W.; Wong, M. W.; Andres, J. L.; Head-Gordon, M.; Replogle, E. S.; Pople, J. A. *Gaussian 98*, revision A.5; Gaussian, Inc.: Pittsburgh, PA, 1998.
(18) Tomoda, S.; Kimura, K. *Chem. Phys*. **1983**, *82*, 215.
(19) Barnett, R. N.; Landman, U. *J. Phys. Chem*. **1997**, *101*, 164.